Proc. Schl. Eng. Tokai Univ., Ser. E
36 (2011) 15-20

Method for Estimating the Maximum Permeation Range of Suspension Grout in Soils

by

Shigeo HONMA[*1] and Walid El KAMASH[*2]

(Received on Mar. 24, 2011 and accepted on Jun. 8, 2011)

Abstract

The permeation mechanism of suspension grouts in soils was investigated by a Kozeny-Carman analysis, and a method for determining the permeability was developed. Laboratory experiments were carried out to investigate the hydrodynamic properties of the grout, the pressure gradient at the onset of flow, and the subsequent process of permeation. The pore-liquid pressure distribution was measured for a one-dimensional vertical sand column and a three-dimensional spherical domain. Based upon both the theoretical and experimental studies, a method for estimating the maximum permeation distance of suspension grouts in soils is shown.

Keywords: Grouting, Ground improvement, Permeability, Non-Newtonian fluid flow through porous material

1. Introduction

A widely used method for improving poor ground involving solidification and stabilization is to inject grout into the foundation. The materials which are employed for this purpose include cement, clay-bentonite solidifying agents, chemicals of various sorts, and mixtures of these, depending on the particular needs and characteristics of the foundation. Cement and clay-bentonite solidifying agents, which are classified as perpetual solidifying grouts, are suspension grouts, consisting of fine particles suspended in solution. Rheologically, they are non-Newtonian fluids with an initial shear strength, that is, yield stress. When a grout of this type is injected into a soil, its flow ceases as soon as a balance is attained between the pressure gradient in the grout and the resistance to shear in the permeation zone.

In this paper, fundamental relationships between the properties of a porous material, such as soil, and the hydrodynamics of non-Newtonian grouts are derived on the basis of a Kozeny-Carman analysis; and a method for determining the permeability is developed. Measurements are made to investigate the mobility characteristics for the different types of suspension grouts. Based on this investigation, laboratory experiments are carried out to confirm the permeability of the suspension grouts, as well as their maximum permeation range within sandy soil.

*1 Professor, Department of Civil Engineering
*2 Assistant Professor, Department of Civil Engineering, Jazan University, Kingdom of Saudi Arabia

2. Flow of a non-Newtonian fluid in a porous material

Flow of a Newtonian fluid through a porous material is empirically governed by Darcy's law. For one-dimensional flow through a saturated porous material, the Darcy equation is

$$Q = KiA \tag{1}$$

where Q is the rate of permeation; K is the permeability of the porous material; $i = dh/dx$ is the hydraulic gradient; and A is the cross-sectional area for permeation. The permeability K incorporates many important factors describing the situation: the complicated flow path through the porous material, the surface state of the particles, the particle density, the degree of saturation, and all of the fluid properties. For a porous material that is, ideally, an assemblage of granular particles, the Kozeny-Carman equation expresses the relationship between these various factors[1,2]:

$$K_N = \frac{\gamma_N C_S e^3 S^3}{\mu_N (1+e) S_0^3} \tag{2}$$

where K_N is the permeability of the medium for the Newtonian fluid; γ_N and μ_N are the weight per unit volume and the dynamic viscosity of the Newtonian fluid, respectively; e is the void ratio of the medium; S is the

saturation; S_0 is the specific wetted surface-area of the granular assemblage; and C_S is the shape factor of the pores in the medium (or the particles).

Using the Kozeny-Carman analysis, the relationship between K and various determinative factors of a non-Newtonian pore fluid with yield stress τ_y are investigated hereafter. Suspension grouts, such as cement and clay-bentonite mixtures, normally have similar hydrodynamic properties to Bingham fluids. The average velocity of a Bingham fluid through a thin tube of radius R is given by[3)]

$$V_{av}=\frac{\gamma_B i R^2}{8\mu_B}\left[1-\frac{8}{3}\frac{\tau_y}{\gamma_B iR}+\frac{16}{3}\left(\frac{\tau_y}{\gamma_B iR}\right)^4\right] \tag{3}$$

where, γ_B is the weight per unit volume of the Bingham fluid; μ_B is the viscosity beyond the yield stress of the Bingham fluid; τ_y is the yield stress; and i is the hydraulic gradient in the tube. When applying Eq.(3) to flow in a porous material, since the flow path passes through an assemblage of particles with various shapes and sizes, the radius R is replaced by both the hydraulic radius R_h of the path of flow and the shape factor C_S, giving

$$q=C_S a\frac{\gamma_B i R_h^2}{2\mu_B}\left[1-\frac{4}{3}\frac{\tau_y}{\gamma_B iR_h}+\frac{1}{3}\left(\frac{\tau_y}{\gamma_B iR_h}\right)^4\right] \tag{4}$$

where a is the cross-sectional area of the flow path, q is the rate of flow, and the hydraulic radius is $R_h=\pi R^2/2\pi R=R/2$. If the flow path through the porous material is thought of as a bundle of thin tubes, and the total cross-section of the material is A, then the average cross-sectional area through which the fluid passes is

$$A_f=AnS=A\frac{e}{1+e}S \tag{5}$$

for a medium with porosity n.

Next, let us consider a flow channel packed with soil particles, as depicted in Fig.1. If V_s is the volume of the solid soil particles, and S_0 is the specific wetted surface, then $PL=S_0V_s$, where P is a wetted perimeter of the channel and L is the length. In terms of the void ratio, e, the pore volume is $A_fL=V_f=eV_sS$. Therefore, the hydraulic radius is given by

$$R_h=\frac{eV_sS}{S_0V_s}=\frac{eS}{S_0} \tag{6}$$

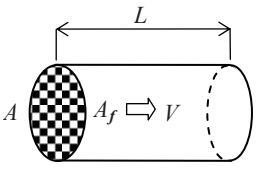

Fig.1 A flow channel filled with soil particles.

Substituting Eq.(6) into Eq.(4), and setting a in Eq.(4) equal to A_f from Eq.(5), gives the total rate of flow:

$$Q=\frac{C_SA\left(\frac{e}{1+e}\right)S\gamma_B i\left(\frac{eS}{S_0}\right)}{\mu_B}\left[1-\frac{4}{3}\left\{\frac{\tau_y}{\gamma_B i\left(eS/S_0\right)}\right\}+\frac{1}{3}\left\{\frac{\tau_y}{\gamma_B i\left(eS/S_0\right)}\right\}^4\right] \tag{7}$$

and relating Eq.(7) to Darcy's law thus gives an equation for the permeability of a porous material with respect to a Bingham fluid:

$$K_B=\frac{\gamma_B C_S e^3S^3}{\mu_B(1+e)S_0^2}\left[1-\frac{4}{3}\left(\frac{\tau_yS_0}{\gamma_B ieS}\right)+\frac{1}{3}\left(\frac{\tau_yS_0}{\gamma_B ieS}\right)^4\right] \tag{8}$$

By way of confirmation, if $\gamma_B=\gamma_N$, $\mu_B=\mu_N$ and $\tau_y=0$ are substituted into Eq.(8), then K_B exactly coincides with the permeability, K_N, for a Newtonian fluid, as given by Eq.(2).

Since a Bingham fluid flowing through a porous material has a yield stress, flow cannot occur below a certain hydraulic gradient. For this critical hydraulic gradient, i_c, at the onset of flow of a Bingham fluid, the term inside the square bracket on the right-hand side of Eq.(8) must be zero and, therefore, i_c is calculated from

$$i_c=\frac{\tau_yS_0}{\gamma_B eS} \tag{9}$$

Here, the specific wetted surface S_0 plays an important role in the onset and cessation of flow. However, if the yield stress τ_y and the unit weight γ_B of the Bingham fluid are found, together with the void ratio e and the saturation S, of the porous medium, then, if the critical hydraulic gradient i_c is measured experimentally, S_0 can be directly evaluated from Eq.(9). Figure 2 shows the relationship between the hydraulic gradient and the permeability of a Bingham pore fluid, in which K_{B0} indicates the first term of Eq.(8) . It is shown that the magnitude of K_B is influenced by τ_y as hydraulic gradient approaches to the critical value.

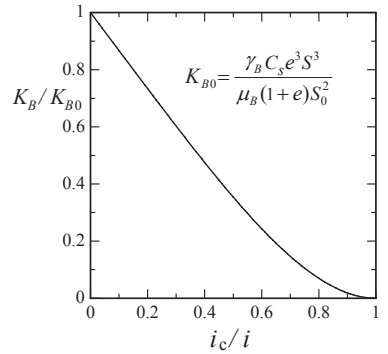

Fig.2 Relationship between the hydraulic gradient and the permeability of a Bingham pore fluid.

3. Experimental investigation

3.1 *Hydrodynamic properties of suspension grouts*

Three types of suspension grouts with various solid-water ratios were prepared. A 1% (W/W) polycarboxylic dispersing agent was added to the Portland cement (mean particle diameter (M.P.D.): 25 μm) and microfine cement[4] (M.P.D.: 4 μm) to prevent segregation of the suspensions. Rotational viscometer tests were then carried out for all three suspensions. Figure 4 illustrates the flow curves of the tests and shows that the grouts can be considered as a Bingham fluid with a yield stress (constitutive equation: $\tau-\tau_y=\mu_B D$). In each case, the yield stress τ_y and the dynamic viscosity beyond the yield stress μ_B increased as the solid-water ratio increased. Changes in the yield stress and dynamic viscosity from increasing the unit mass density of the suspensions are shown in Fig.3. As the microfine cement grout has τ_y and μ_B that are one order of magnitude smaller than those of the other suspensions, microfine cement grout is thought to give better permeability when injected into soils.

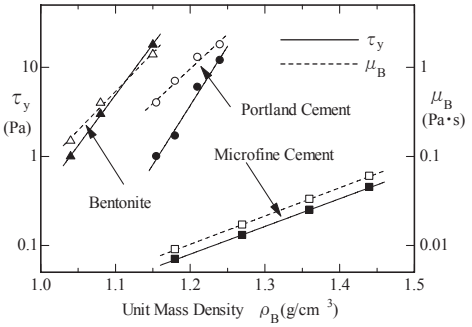

Fig.3 Change of yield stress and viscosity.

3.2 *Seepage resistance of suspension grouts in soils*

Based on the aforementioned discussion and measurements, laboratory experiments were conducted to investigate the seepage resistance of the suspension grouts. The experimental set-up is depicted in Fig.5, and consists of an air-pressurized grout supply tank connected to a seepage test pipe packed with fine sand (grain size: 0.425~0.25 mm). Pressure gauges were installed on the both sides of the specimen to measure the pressure gradient.

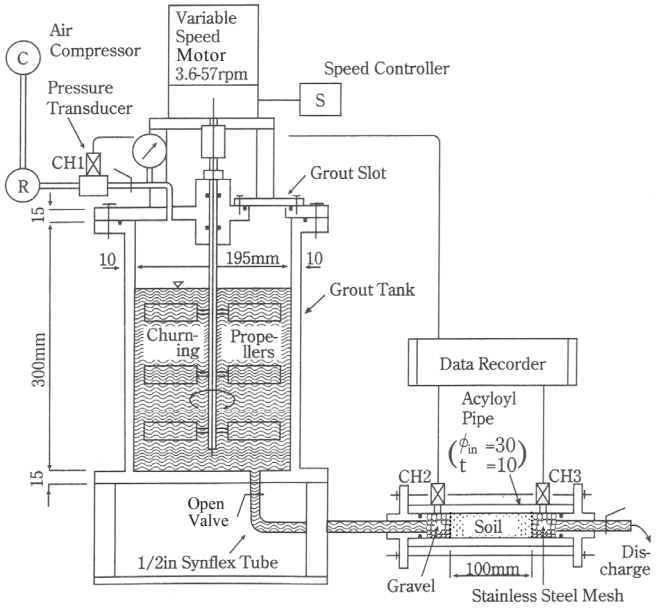

Fig.5 Experimental setup for measuring seepage resistance.

After saturating the sand specimen with one of the prescribed grout mixtures, the air-pressure was increased in 10 kPa increments up to 100 kPa and by 50 kPa increments thereafter, during which the amount of discharge was measured. For the bentonite suspensions and the microfine cement grouts, these experiments were implemented successfully; however, some of the Portland cement grouts plugged up the screen mesh and a considerable degree of segregation was observed.

Excluding these plugged cases, Fig.6 shows the relationships between the pressure gradient ($I=\Delta p/L$) and average velocity through the specimens ($V=Q/A$). It can be seen that the grout starts to permeate once a certain limiting pressure gradient has been exceeded, and therefore, it is confirmed that the critical pressure gradient I_c does indeed

Table 1 Hydrodynamic properties of microfine grout.

C:W	e	γ_B (kN/m^3)	τ_y (Pa)	μ_B (Pa·s)	I_c (MPa/m)	i_c
1:1	0.85	14.0	0.45	0.05	0.85	60.7
1:2	0.87	12.5	0.15	0.016	0.30	24.0
1:3	0.90	11.7	0.08	0.010	0.15	12.8

Note: μ_w= 0.001 Pa·s

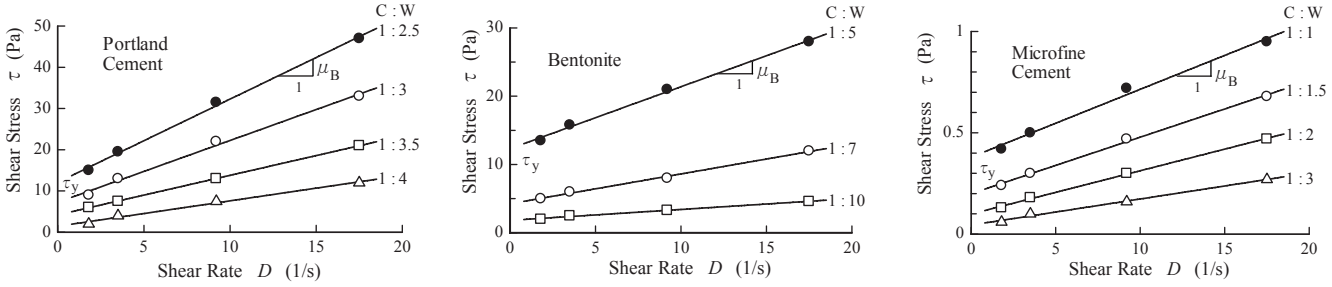

Fig.4 Flow curves for the grouts, found using rotational viscometer tests.

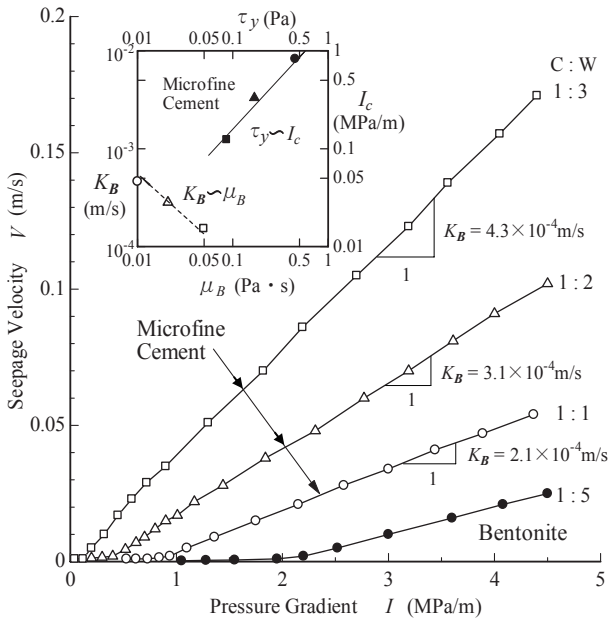

Fig.6 Relationship between V and I for the permeating grouts.

exist. Values for the critical pressure and hydraulic gradients for the microfine cement grouts are given in Table 1, which indicates that the critical pressure gradient I_c and the critical hydraulic gradient i_c increase as the solid-water ratio increases. It can also be seen from Fig.6 that there exists proportionality between τ_y and I_c and inverse proportionality between K_B and μ_B. These relationships agree with the theoretical observations described in Section **2**.

Using the critical hydraulic gradients and the hydrodynamic properties of the grouts shown in Table 1, the wetted surface area, S_0, of the sand specimen can be evaluated from:

$$S_0 = \frac{\gamma_B e S}{\tau_y} i_c = \frac{eS}{\tau_y} I_c \tag{10}$$

The mean value of S_0 is thus calculated as 1.65×10^6 m^{-1}, and

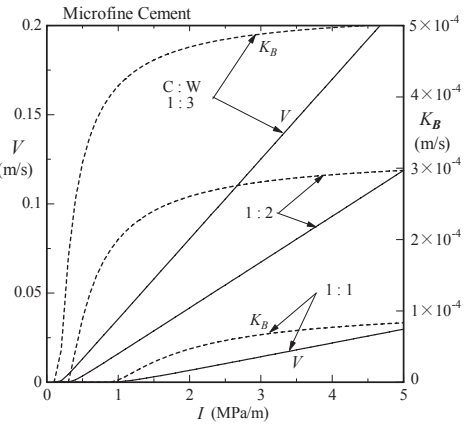

Fig.7 Calculated results for the change of K_B and V with the pressure gradient I.

since the hydraulic conductivity of the sand was found to be $K_N = 1.5\times10^{-3}$ m/s, the shape factor of the packed sand can be evaluated from Eq.(2):

$$C_S = \frac{K_N \mu_N (1+e) S_0^3}{\gamma_N e^3 S^3} = 1360 \tag{11}$$

With all of the physical values in Eq.(8) determined, both the change of permeability K_B and permeation velocity $V = K_B I/\gamma_B$, with the pressure gradient I, can be ascertained. The results are shown in Fig.7 and it can be observed that the K_B values initiate and rise rapidly at the critical pressure gradients, before settling to constant values. On the other hand, the average seepage velocities exhibit a linear increase for $I > I_c$, and, in general, become coincident with the experimental results shown in Fig.6.

4. Maximum permeation range of the suspension grouts in soils

From the results already discussed, it is a reasonable supposition that the flow of suspension grouts in soils ceases as

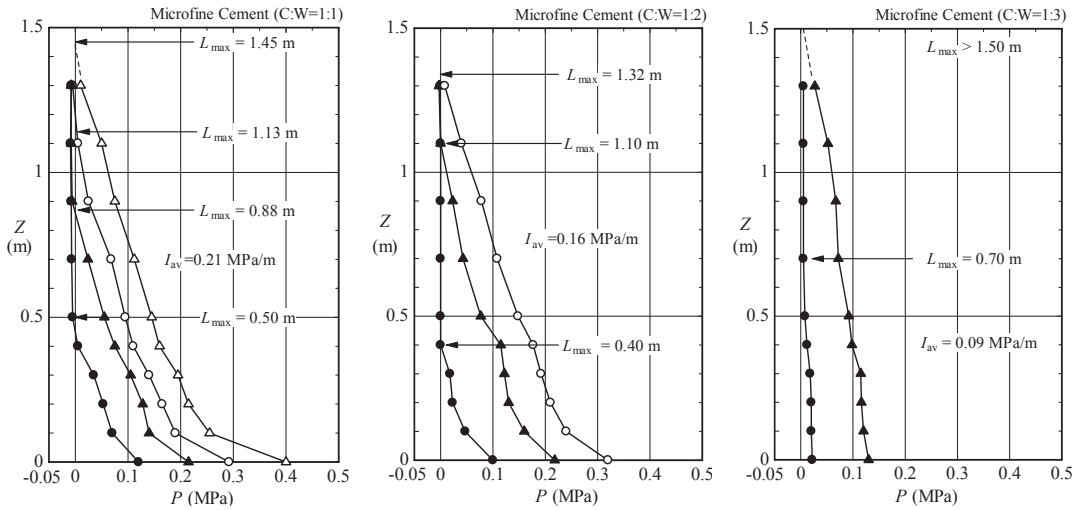

Fig.8 Experimental results showing the pore-liquid pressure distribution in a vertical sand column.

soon as the pressure gradient in the grout reaches the critical state, thereby limiting the range of permeation. Laboratory injection experiments were carried out to confirm this phenomenon using the apparatus shown in Fig.5, but here the short sand specimen was replaced with a 1.5-m vertical sand column. Pressure gauges were installed along this column at intervals of 0.1 m from the bottom, to a height of 0.5 m, and at 0.2-m intervals thereafter.

The prescribed mixtures of the microfine grouts were supplied from the bottom of the column by increasing the pumping pressure in 0.1 MPa increments. Figure 8 shows the distribution of the pore-liquid pressures for three cement-water ratios. Pressure drops are observed at $Z=0$, due to the pressure gauge at this position being outside the lower screen; otherwise, throughout the permeation zone, an almost linear distribution developed. This implies that a balance was attained between the pressure gradient in each grout and the resistance to shear in the permeation zone. The locations indicated by arrows show the maximum permeation range for that grout estimated from the critical pressure gradient.

The experimental critical pressure gradients were somewhat smaller than the theoretically expected values. This is attributed to severance (split-off) of the grout through permeation and also to imperfect contact between the permeating grout and the measurement surface of the pressure gauge.

Figure 9 shows the maximum permeation range of the microfine cement grout within a spherical domain, based upon the critical pressure gradient. Using a diagram similar to Fig.9, it is possible to estimate the maximum permeation distance of an injected grout in an actual grouting operation for various cement-water ratios and pumping pressures.

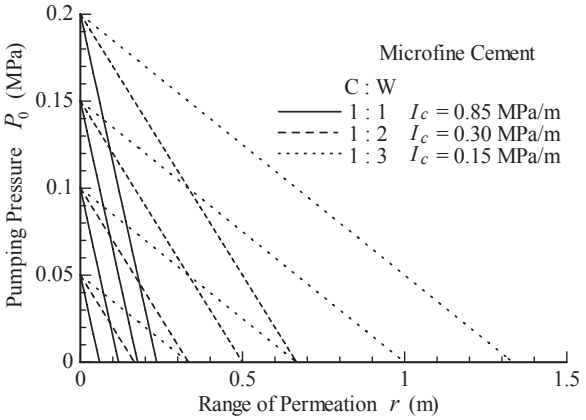

Fig.9 Maximum permeation range in a spherical domain.

Lastly, a laboratory experiment was conducted using microfine cement with the solid-water ratio of 1:2, to simulate a grouting operation. A cylindrical tank, 45 cm in diameter and 60 cm in height, was prepared as shown in Fig. 10. The soil filled was the sieved hill sand of the grain size 0.425~0.25 mm, and the permeability $K=3.1\times10^{-2}$cm/s. An injection pipe and a pair of pressure gauges were positioned at 20 cm from the bottom of the tank. The injection pipe was connected to the grout tank in the same manner as shown in Fig.5, and 20 kPa of air pressure was applied to supply the grout mixtures to the tank. The dry density and void ratio of the filled sand were ρ_d = 1250 kg/m^3, e =1.12, respectively.

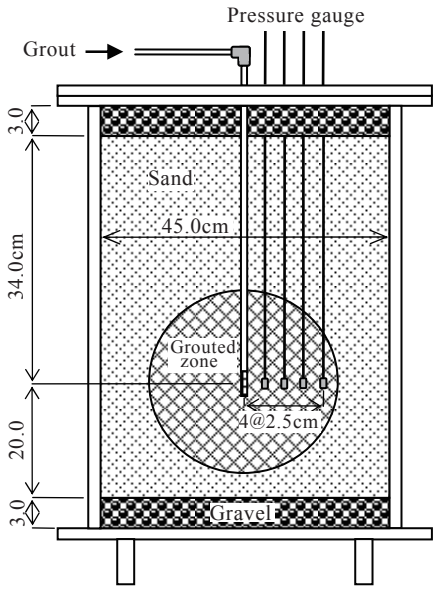

Fig.10 Grouting experiment in a spherical domain.

Figure 11 shows the pressure distribution in the radial direction from the injection point. Under the applied pumping pressure, the permeation ceased after 8 min, at which point an almost linear pressure distribution was observed in the permeation zone. The average pressure gradient for this experiment was 0.23 MPa/m.

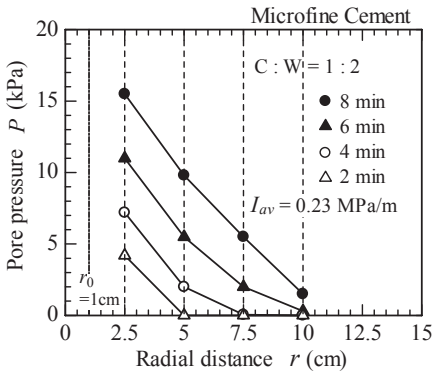

Fig.11 Pressure distribution in a spherical domain.

If a constant pumping rate is applied at the injection point, changes in the pumping pressure and the advancement of the permeating grout front can be also computed. Figure 12 shows the calculated results at an applied pumping rate of

$q = 3 \times 10^{-4}$ m^3/min. It can also be seen from this figure that the pumping pressure increases rapidly in the early stages of pumping, but that this rate of increase slows as time advances. A similar transition is observed in the advancement of the grout front; however, experimental confirmation of this behavior is required in future work.

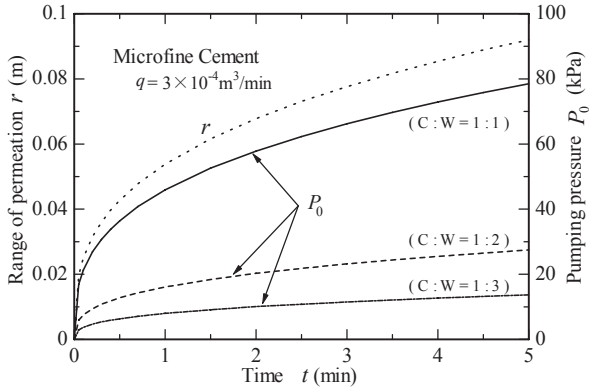

Fig.12 Changes in the pumping pressure and permeation at a constant pumping rate.

5. Conclusions

From the theoretical and experimental investigations presented in this paper, the following two conclusions can be reached regarding the seepage mechanism of suspension grouts in soils:

1) By modeling suspension grouts as a Bingham non-Newtonian fluid with a yield stress, the mobility of the grout is approximated well mechanically. For the interstitial Bingham fluid, the coefficient of permeability through a porous medium can be derived by a Kozeny-Carman analysis. In this analysis, the critical pressure gradient controls the onset of flow, plus the subsequent permeation of the grout injected into a soil.
2) Laboratory grouting experiments, show close correspondence to the calculated theoretical relationships, in terms of the magnitudes of the permeability, pressure distribution and the critical pressure gradient. It is therefore possible when grouting to estimate the maximum permeation range from the physical and hydromechanical properties of the soil and the grout.

References

1) Bear, J. 1972, *Dynamics of fluids in porous media*, American Elsevier.
2) Dullien, F.A.L. 1979, *Porous media*; *Fluid transport and pore structure*, Academic Press.
3) Wilkinson, W.L. 1960, *Non-Newtonian fluids*; *Fluid mechanics, mixing and heat transfer*, Pergamon Press.
4) Shimoda, M., Hayakawa, H. and Hosoda, H., 1982, Basic properties and some applications of superfine granular grouts, *Cement Gijutu Nenpo*, 36, pp.505−508.
5) Honma, S. 1993, A study on the seepage resistance of suspension-type grouts in soils, *Int. Chemical Eng.*,Vol.33, pp.315−325.
6) Honma, S. and Inada. M., 1996, The seepage resistance of suspension grouts in soils, *Proc. of* 2nd *Int. Conference on Ground Improvement Geosystems*, pp.37−40.
7) Honma, S., 1996, Mobility and permeability of suspension-type grouts, *Proc. of the School of Eng., Tokai Univ.*, Vol.XXI, pp.37-46.